

Interplay between Fermi surface topology and ordering in URu₂Si₂ revealed through abrupt Hall coefficient changes in strong magnetic fields

Y. S. Oh¹, Kee Hoon Kim¹, P. A. Sharma², N. Harrison², H. Amitsuka³, and J. A. Mydosh⁴

¹*CSCMR & FPRD, School of Physics and Astronomy,
Seoul National University, Seoul, 151-747, South Korea*

²*NHMFL, Los Alamos National Lab., MS E536, Los Alamos, NM 87545, USA*

³*Graduate School of Science, Hokkaido University, N10W8 Sapporo 060-0810, Japan*

⁴*Institute of Physics II, University of Cologne, 50937 Cologne, Germany*

Temperature- and field-dependent measurements of the Hall effect of pure and 4 % Rh-doped URu₂Si₂ reveal low density (0.03 hole/U) high mobility carriers to be unique to the ‘hidden order’ phase and consistent with an itinerant density-wave order parameter. The Fermi surface undergoes a series of abrupt changes as the magnetic field is increased. When combined with existing de Haas-van Alphen data, the Hall data expose a strong interplay between the stability of the ‘hidden order,’ the degree of polarization of the Fermi liquid and the Fermi surface topology.

PACS numbers: 71.45.Lr, 71.20.Ps, 71.18.+y

When observed, quantum oscillatory effects such as the de Haas-van Alphen (dHvA) effect provide a definitive measure of the Fermi surface topology in metals. There are some situations, however, in which quantum oscillatory effects lose their sensitivity— at very low magnetic fields, through a thermally driven phase transition or, more recently, at a quantum phase transition. As the predictive power of Hall theory improves, the Hall effect is becoming increasingly recognized as a viable alternative for understanding Fermi surface changes in *f*-electron antiferromagnets and ferromagnets tuned close to quantum criticality [1, 2]. Any knowledge of the extent to which the *f*-electrons contribute to the Fermi surface topology is of crucial importance for understanding the nature of the ordering and the fate of the heavy quasiparticles.

In URu₂Si₂, Fermi surface measurements have the potential to assist in the identification of the ‘hidden order’ phase that forms below $T_o \approx 17.5$ K [3, 4]. Even if the order parameter cannot be seen directly, its effect on modifying the Fermi surface topology could provide valuable information on its symmetry breaking properties. Strong correlations make this all the more challenging by both restricting the observable temperature (T) range of quantum oscillations to $T \ll T_o$ [5] and inhibiting the predictive ability of band structure calculations. Under strong magnetic fields ($B \approx \mu_0 H$), the HO phase is destabilized through a cascade of first order phase transitions between consecutive field-induced phases (see Fig. 1) [6]. A strengthening of the correlations in the vicinity of a putative field-tuned quantum critical point at $B_m \approx 37$ T [7] is identified as a likely factor, although the changes in the Fermi surface topology have not been addressed.

In this letter, we show that Hall effect measurements extended to high magnetic fields reveal the anomalous contribution to become weak at low T . The remaining orbital Hall effect uncovers an intricate level of interplay between the Fermi surface topology and the stability of the various phases of pure and 4 % Rh-doped URu₂Si₂ [7]. At

low H and T , the enhancement of the Hall coefficient and Hall angle [8, 9, 10] shows that the otherwise large Fermi surface is reconstructed into small high mobility pockets below T_o in URu₂Si₂: a finding that is ubiquitous among imperfectly-nested itinerant forms of broken translational symmetry groundstates [11, 12, 13, 14] and consistent with low T dHvA measurements on URu₂Si₂ [5]. This groundstate is then destabilized when a magnetic field causes two of the high mobility pockets to become spin polarized, ultimately leading to its destruction at ≈ 35 T. Intermediate larger and strongly polarized Fermi surfaces appear in phases II, III and V before a fully polarized unreconstructed Fermi surface is achieved beyond ≈ 39 T with 1 hole/U and $1.5 \mu_B/U$.

Single crystals of URu₂Si₂ and U(Ru_{0.96}Rh_{0.04})₂Si₂ (Rh 4 %) are grown using the Czochralski method and cut into standard Hall bar geometries with 6-wire contacts in the tetragonal *ab* plane. The longitudinal and transverse voltage signals are detected simultaneously using a pulsed magnetic field of ~ 100 ms duration applied along *c*-axis up to 45 T. Special care is taken to obtain Hall coefficient data under isothermal conditions during the pulse by confirming consistency of the resistivity and phase boundaries with measurements made in the static magnet [7]. The ability to reverse the polarity of the pulsed magnetic field in-situ between pulses enables the diagonal ρ_{xx} and off-diagonal (Hall) ρ_{xy} to be determined accurately. Resistivities measured at positive and negative B are subtracted and added to extract the two components.

Figure 1(c)-(f) shows typical ρ_{xx} and ρ_{xy} data for both pure and 4 % Rh-doped URu₂Si₂ obtained at low temperatures. The ρ_{xx} data are qualitatively similar to published ρ_{zz} data [6, 7]. In contrast to the original Hall measurements of Bakker *et al.* up to 40 T [15], the present ρ_{xy} data are linear in B within each high magnetic field phase, and also within the HO phase for $B \lesssim 26$ T (we discuss the region $26 \lesssim B \lesssim 35$ T below). This is true at

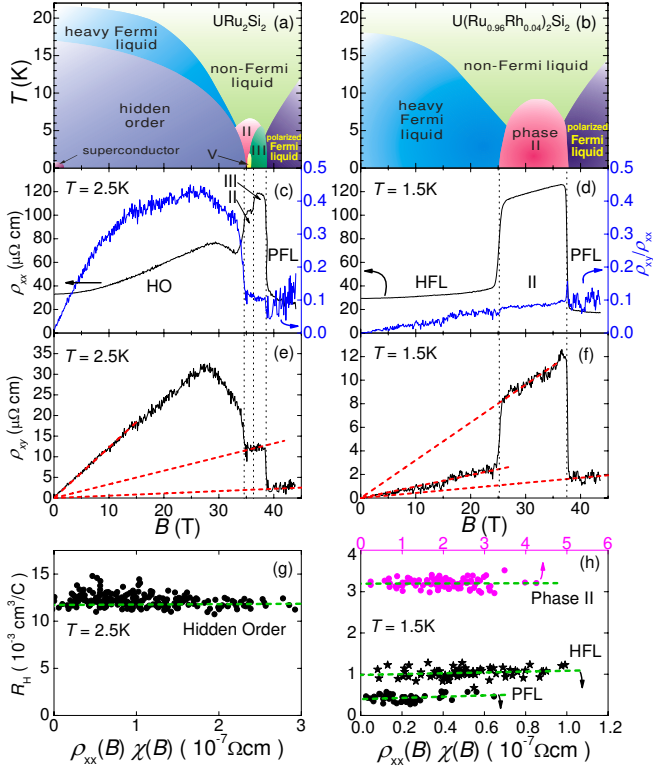


FIG. 1: Left axes: (a)&(b) Phase diagram [6, 7], (c)&(d) longitudinal resistivity ρ_{xx} and (e)&(f) Hall resistivity ρ_{xy} (g)&(h) linear extrapolations to estimate the anomalous Hall contribution of URu_2Si_2 at $T = 2.5$ K and $\text{U}(\text{Ru}_{0.96}\text{Rh}_{0.04})_2\text{Si}_2$ at $T = 1.5$ K, respectively. Red dotted linear lines passing through the origin are guides for the eye. Green dotted lines are linear extrapolations as explained in texts. Right axes: (c)&(d) ρ_{xy}/ρ_{xx} for both compounds.

all temperatures $\lesssim 5$ K and for both samples in Figs. 2(a) and 3(a), enabling the Hall coefficient $R_H \equiv \rho_{xy}/B$ to be reliably extracted in Figs. 2(b) and 3(b). Temperature control and isothermal conditions are important factors in ensuring the reliability of the present measurements. The ability to stabilize T over a considerable range also enables us to ascertain the anomalous Hall coefficient R_{aH} as a relatively weak effect when compared to the orbital contribution in the low T limit.

Empirically, $R_{aH}(T) \approx C_a \rho_{xx}(T) \chi(T)$ in heavy fermion metals [2, 16], where C_a is a constant. The intrinsically narrow quasiparticle bandwidth approaching H_m implies that even the orbital contribution will be T -dependent (i.e. see Figs. 2 & 3), thus requiring a modified analysis. Here, we evaluate the anomalous contribution by plotting $R_H(B)$ versus $\rho_{xx}(B) \chi(B)$ at fixed values of T when $\chi(B) = \partial M(B)/\partial H(B)$ and $B \approx \mu_0 H$, yielding a constant slope C_a within each phase as shown in Figs. 1(g) and 1(h). Within the HO phase at $T=2.5$ K, $C_a \approx 0.0420 \text{ T}^{-1}$ and the resultant R_{aH} is less than 2% of the orbital contribution. C_a cannot be extracted reliably

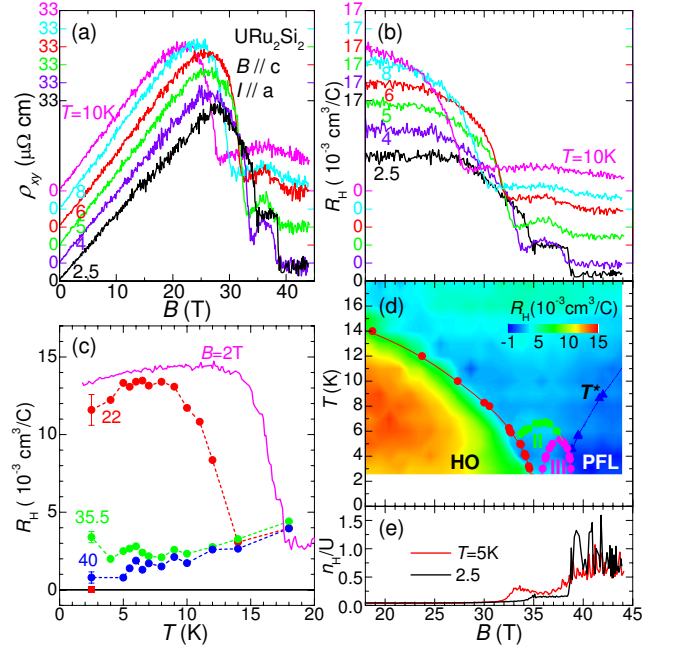


FIG. 2: (a) ρ_{xy} and (b) $R_H \equiv \rho_{xy}/B$ of URu_2Si_2 at selected temperatures. (c) Temperature dependence of R_H at selected B and typical error bars of R_H in each phase region. R_H at 2 T (magenta line) is obtained from the temperature sweep using a superconducting magnet. The red square represents the estimated anomalous contribution in the HO state, which is less than 2% of the measured R_H . (d) The B - T contour plot of R_H and published phase boundaries (solid symbols) [6]. (e) The effective carrier density, $n_H \equiv -1/eR_H$ at $T = 2.5$ and 5 K.

for the other phases of pure URu_2Si_2 . However, for the 4% sample at $T=1.5$ K, we obtain $C_a \approx 0.1013$, 0.0027 , and 0.1473 T^{-1} for the heavy Fermi liquid (HFL), phase II and polarized Fermi liquid (PFL) regimes respectively, implying that R_{aH} contribution is always less than 7% of R_H for $T \lesssim 3$ K. This serves as an upper limit for the error involved in extracting values of n_H from R_H at the lowest temperatures.

In this respect, the 4% Rh-doped sample serves as a ‘reference’ sample for which there is no HO at low fields—the only phase that survives Rh-doping is phase II. The high sensitivity of the Fermi surface transitions to perturbations in the electronic structure may explain the complete suppression of the HO phase in the Rh 4% sample at low fields as shown in Fig. 1(b). 4% Rh-doped URu_2Si_2 nevertheless has the advantage of having its unreconstructed Fermi surface probed by Hall effect measurements at the lowest temperature ($T \ll T_{HO}$) where the anomalous contribution is smallest. The low magnetic field value of R_H corresponds to $n_H \approx 0.5$ holes per U, which is significantly larger than the additional ≈ 0.08 $4d$ -electrons per U introduced by Rh substitution on the Ru sites. This greatly reinforces previous assump-

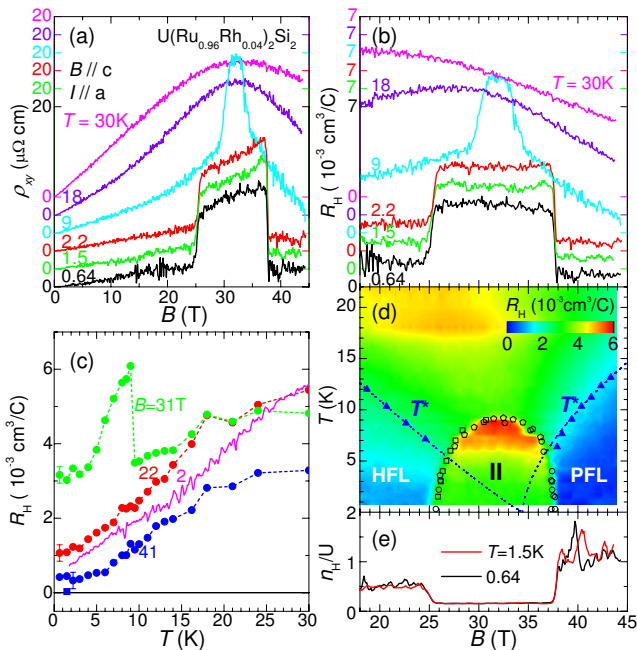


FIG. 3: (a) ρ_{xy} and (b) R_H of $U(\text{Ru}_{0.96}\text{Rh}_{0.04})_2\text{Si}_2$ at selected temperatures. (c) Temperature dependence of R_H at selected B and typical error bars of R_H in each phase region. The blue square represents the estimated anomalous contribution in the PFL region, which is less than 7 % of the measured R_H . (d) The B - T contour plot of R_H and published phase boundaries (open circles) [7]. (e) The effective carrier density, $n_H \equiv -1/eR_H$ at $T = 0.64$ and 1.5 K.

tions that low T value of $n_H \equiv -1/R_H e \approx 0.03/U$ within the HO phase of pure URu_2Si_2 is primarily due to the opening of a gap over the majority of the Fermi surface [8, 9, 10]. This result is robust against differences in residual resistivity and sample quality.

One remarkable feature of the data presented in Fig. 1 is that the tangent of the Hall angle estimated from $\tan \theta = \rho_{xy}/\rho_{xx}$ is strongly enhanced *only* within the HO phase, indicating the existence of high mobility carriers which cause the product $\omega_c \tau$ (where ω_c is the cyclotron frequency and τ is the relaxation time) to become much larger than elsewhere in the phase diagram. The development of high mobility carriers is a ubiquitous feature of itinerant order parameters that break translational symmetry (i.e. spin- and charge- and density waves) in which imperfect-nesting leads to the creation of small pockets [11, 12, 13, 14]. On considering the mean free path $l = \tau v_F$, where $v_F = \hbar k_F/m^*$ is the orbitally averaged Fermi velocity, $k_F = \sqrt{2eF/\hbar}$ is the mean Fermi radius and F is the dHvA frequency, the carrier mobility becomes $\omega_c \tau/B \equiv e\tau/m^* = el/\hbar k_F$. Thus, high mobilities within the HO phase can be explained simply by the creation of small pockets with small k_F values, without needing to consider changes in τ or l at T_0 , or d -wave

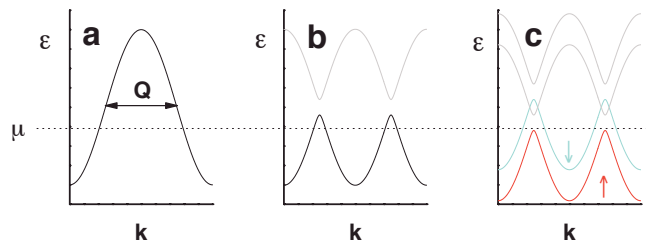


FIG. 4: Schematic cross-section in k -space through a hypothetical hole band. Broken translational symmetry (\mathbf{Q}) can cause such a band (a) to be reconstructed into small pockets with a Dirac-like dispersion (b) which are then easily polarized by a magnetic field (c).

order parameters [17].

dHvA experiments within the HO phase at $T \ll T_0$ provide direct evidence for small high mobility pockets [5]. The largest of these (α) has double the mobility $e\tau/m^* \approx 0.12\text{ T}^{-1}$ of the others (β and γ) and a volume that agrees with n_H obtained from the Hall effect measurements. Such small pockets, and subsequently the stability of order parameter responsible for their creation, are vulnerable to perturbations. The intrinsically large effective masses in itinerant f -electron metals enables such pockets to be easily polarized by a magnetic field, as shown schematically in Fig. 4(c). The polarization field B_p can be estimated directly from the dHvA data by equating the Fermi liquid, $\varepsilon_F = \hbar e F/m^*$ and Zeeman $h = g_z \sigma \mu_B B$ (band splitting) energy scales. Here, F is proportional to the cross-sectional area of an orbit A_k in reciprocal space by way of the Onsager relation $F = \hbar A_k/2\pi e$ while $g_z \sigma \approx 1.3$ is the product of the g -factor and spin determined from field orientation-dependent experiments [18]. This yields $B_p \approx 120, 25$ and 35 T for the known α, β and γ carrier pockets, respectively [5]. Thus, one spin component of the heaviest β pocket, is expected to become depopulated well within the HO phase, while that of the γ pocket is depopulated at the same field $B_c \approx 35\text{ T}$ where the transition out of the HO phase into phase II is observed (see Fig. 1 (a)). As a consequence of such a depopulation, the chemical potential μ must re-equilibrate itself amongst the remaining pockets, leading to changes in their sizes and net observable changes in R_H . Indeed, as observed in Figs. 1(e) & 2(b), once one spin component of the heaviest β pocket becomes depopulated beyond $\approx 25\text{ T}$, ρ_{xy} , and consequently, R_H starts a downward trend. Since R_H is primarily due to the α pocket of holes, the downward trend suggests that it is the up spin component of a hole-like β pocket that becomes depopulated contributing its carriers to α . This downward trend then rapidly accelerates beyond $\approx 34\text{ T}$ as B_p for the γ pocket is approached, indicating it to be another hole pocket that becomes depopulated. Close inspection of Fig. 2(b) reveals that the

drop in R_H overshoots that subsequently observed within phases II and III, suggesting that depopulation of the β and γ pockets factors into the destruction of the HO phase. If stability of the HO phase requires an optimum value of translational vector \mathbf{Q} that gaps most of the Fermi surface, this \mathbf{Q} will no longer be optimal once μ begins to change, exacerbating the destabilization of the HO phase by the Zeeman effect.

The destruction of the HO phase is accompanied by an increase in n_H from $\sim 0.03/U$ inside HO to $\sim 0.15/U$ inside phase II, suggesting that a significant fraction of the unreconstructed Fermi surface is recovered. The appearance of such a large Fermi surface will cause the Hall effect to become dominated by lower mobility carriers, thus explaining the restoration of $\tan\theta$ to values comparable to that of the complete unreconstructed Fermi surface. Surprisingly, neither the additional 0.08 electrons per U nor the disorder introduced by charged impurities in 4 % Rh-doped URu_2Si_2 appears to have a detrimental effect on the stability of phase II. The collapsing energy scale of the Fermi liquid temperature of the unreconstructed Fermi surface associated with the field-induced correlations could be playing a role in making this phase more robust to disorder [6, 7, 19]. This would be especially true were the phase to involve local moment ordering of XY electric quadrupolar degrees of freedom [20, 21]. Similarities in the value of both R_H (Figs. 2 and 3 (b) & (c)) and M_z within phase II [20, 22] in pure and Rh-doped URu_2Si_2 suggest that the precise degree of polarization of the Fermi liquid is an intrinsic property of the order parameter.

In both pure and 4 % Rh-doped URu_2Si_2 , the destruction of the field-induced phases is followed by a complete polarization of the unreconstructed quasiparticle bands [19] whereupon ordering is no longer possible. The saturation of the magnetization at $\sim 1.5\mu_B/U$ within the polarized Fermi liquid (PFL) state is accompanied by an increase in R_H to a value corresponding to $0.9 \pm 0.3/U$ and $1.1 \pm 0.2/U$ in pure and 4 % Rh-doped URu_2Si_2 respectively. The realization of a carrier density of $\approx 1/U$ is consistent with the entropy recently observed in heat capacity measurements of the polarized bands [19].

In conclusion, a clear picture of the interplay between the Fermi surface topology, degree of polarization of the Fermi liquid and the stability of the HO and field-induced order parameters is now starting to emerge in URu_2Si_2 . At low magnetic fields, T_0 is accompanied by a significant gapping of the majority of the Fermi surface, leading to a reduction in the electronic heat capacity and Hall number. An itinerant density-wave order parameter of the type inferred from thermal conductivity measurements [23] would provide a mechanism by which small pockets of highly mobile carriers could be produced in Fig. 4. Evidence for a low density of highly mobile carriers appears not just in the measurements of the Hall angle, but also in the Nernst [10] and dHvA effects [5].

The intrinsically heavy masses of these pockets (compared to regular band electrons) makes them vulnerable to polarization by a magnetic field (i.e. like in Fig. 4(c)), which subsequently destabilizes the HO phase. The polarization of at least two of the three pockets can both be predicted from existing dHvA measurements [5, 18] and observed directly in the Hall effect, ultimately factoring into the destruction of the HO phase at ≈ 35 T. Phases II, III and V involve some form of intermediate ordering that accommodates a partial polarization of the f -electrons and partially gapped quasiparticle bands. Finally, ordering of any type is prohibited once the unreconstructed quasiparticle bands are completely polarized [19], yielding a simple polarized ≈ 1 hole/U metal at $B \gtrsim 39$ T.

This work is supported by Korean government through NRL program (M10600000238) and through KRF (KRF-2005-070-C00044). YSO is supported by the Seoul R&BD Program, KHK by KOSEF through CSCMR, and JAM by the A. von Humboldt Foundation. The work at NHMFL is performed under the auspices of NSF, DOE and Florida State.

-
- [1] P. Coleman, C. Pépin, Q. Si, and R. Ramazashvili, J. Phys. Condens. Matter **13**, R723 (2001); M. R. Norman, Phys. Rev. B **71**, 220405 (2005); A. Yeh *et al.*, Nature **419**, 459 (2002); S. Sachdev, Science **288**, 475 (2000); H. Löhneysen, J. Magn. Magn. Mat. **200**, 532 (1999); P. Gegenwart *et al.*, Phys. Rev. Lett. **89**, 056402 (2002); G. R. Stewart, Rev. Mod. Phys. **73**, 797 (2001); S. A. Grigera *et al.*, Science **294**, 329 (2001); *ibid.*, **306**, 1154 (2004).
 - [2] S. Paschen *et al.*, Nature **432**, 881 (2004).
 - [3] T. T. M. Palstra *et al.*, Phys. Rev. Lett. **55** 2727 (1985).
 - [4] P. Chandra *et al.*, Nature **417**, 831 (2002).
 - [5] H. Ohkuni *et al.*, Philos. Mag. B **79**, 1045 (1999).
 - [6] K. H. Kim *et al.*, Phys. Rev. Lett. **91**, 256401 (2003).
 - [7] K. H. Kim *et al.*, Phys. Rev. Lett. **93**, 206402 (2004).
 - [8] J. Schoenes *et al.*, Phys. Rev. B **35**, 5375 (1987).
 - [9] A. LeR Dawson *et al.*, J. Phys.: Cond. Matt. **1**, 6817 (1989).
 - [10] R. Bel *et al.*, Phys. Rev. B **70**, 220501(R)(2004).
 - [11] K. Okajima and S. Tanaka, J. Phys. Soc. Jpn **53**, 2332 (1984).
 - [12] T. Sasaki, S. Endo and N. Toyota, Phys. Rev. B **48**, 1928 (1993).
 - [13] P. M. Chaikin, J. Phys. I (France) **6**, 1875 (1996).
 - [14] U. Beierlein *et al.*, Synth. Met. **103**, 2593 (1999).
 - [15] K. Bakker *et al.*, Physica B **186-188**, 720 (1993).
 - [16] A. Fert and P. M. Levy, Phys. Rev. B **36**, 1907 (1987).
 - [17] K. Behnia *et al.*, Phys. Rev. Lett. **94**, 156405(2005).
 - [18] A. Silhanek *et al.*, Physica B **378-380**, 373 (2006).
 - [19] A. V. Silhanek *et al.*, Phys. Rev. Lett. **95**, 026403 (2005).
 - [20] A. V. Silhanek *et al.*, Phys. Rev. Lett. **96**, 136403 (2006).
 - [21] F. Ohkawa and H. Shimizu, J. Phys.: Cond. Matt. **11**, L519 (1999).
 - [22] N. Harrison, M. Jaime, and J. A. Mydosh, Phys. Rev. Lett. **90**, 096402 (2002).
 - [23] P. A. Sharma *et al.*, Phys. Rev. Lett. **97**, 156401 (2006).